

# Experimental Investigation of Charge Carrier Transport in Organic Thin-Film Transistors with “Buried Surface Layers”

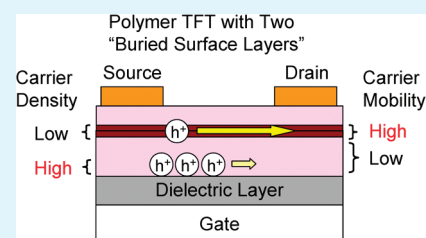
Qingshuo Wei,<sup>†</sup> Kazuhito Hashimoto,<sup>\*,†,‡</sup> and Keisuke Tajima<sup>\*,†,‡</sup>

<sup>†</sup>HASHIMOTO Light Energy Conversion Project, Exploratory Research for Advanced Technology (ERATO), Japan Science Technology Agency (JST)

<sup>‡</sup>Department of Applied Chemistry, School of Engineering, The University of Tokyo, 7-3-1 Hongo, Bunkyo-ku, Tokyo 113-8656, Japan

**ABSTRACT:** We studied how the layers with different transport properties buried inside a semiconductor material affect the characteristics of organic thin film transistors (OTFT) using a well-defined multilayered structure fabricated by a contact film transfer method that we recently developed (ACS Appl. Mater. Interfaces 1, 2660 (2009)). A simple model with the charge distribution in the organic semiconductor film, the mobility dependence on the charge density, and the buried surface layers with a high mobility successfully reproduced the experimental mobility dependence on the thickness of the spin-coated films and the gate voltage. These results demonstrated that charge transport layers located far from the dielectric interface could contribute significantly to the total current in OTFTs.

**KEYWORDS:** organic field-effect transistor, film transfer, charge transport, interfacial property



Organic thin-film transistors (OTFTs) have attracted considerable attention because of their potential application to large-area, mechanically flexible, lightweight, and inexpensive electronic logic circuits.<sup>1</sup> OTFTs are fabricated by depositing organic semiconductors on a dielectric layer either by dry vacuum depositions or solution processes. In general, semiconductors in the deposited films have quite different structures between at the interface and in the bulk part since the surface properties of the substrate have a strong influence on the molecular orientation and the formation of structural defects at the interface.<sup>2–6</sup> Because the charge transport in a OTFT mainly occurs in the vicinity of the dielectric interface, this difference in the charge transport properties inside the semiconductor film could be the main reason for the complications of OTFT behaviors such as strong dependence of the charge mobility on fabrication conditions and the properties of the dielectric materials.<sup>7–9</sup> Although much effort has been made from the theoretical viewpoints, there is still limited experimental investigation on this issue due to the difficulty in the reproducible production of the structures with different charge transport properties in the semiconducting films. If this is possible in a controlled manner, it would give us an experimental tool to understand how they affect the OTFT characteristics.

Recently, we developed a simple “contact film transfer (CFT)” method to transfer semiconducting polymer films upside-down onto dielectric layers in mild conditions.<sup>10–12</sup> This CFT method enables the fabrication of high-performance OTFTs by utilizing the structure formed at the polymer/air interface as the charge transport layer. As the result, the OTFTs prepared by CFT of poly(3-hexylthiophene) (P3HT) film have much higher mobility than those prepared by conventional spin-coating, which can be attributed to high molecular orientation and strong interchain

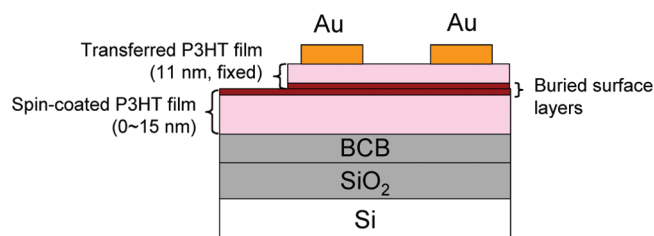


**Figure 1.** Schematic representation of the bottom-gate, top-contact OTFT based on the spin-coated and the transferred P3HT film used in this study.

$\pi$ – $\pi$  interactions of P3HT at the polymer/air interface compared to those at the polymer/substrate interface formed during the spin-coating.<sup>4,11</sup>

In this work, we utilize CFT method to transfer a P3HT film onto another P3HT film that is spin-coated on the dielectric layer. The resulting structure has two surface layers of P3HT originally formed at the polymer/air interfaces but now buried in the middle of the film (Figure 1). These “buried surface layers” have well-oriented edge-on packing and high mobility as suggested in the previous works, and the rest of the film (the bulk part and dielectric/spin-coated film interface) could have a relatively disordered structure and lower carrier mobility.<sup>11</sup> By changing the thickness of the spin-coated P3HT films, the distance of the “buried surface layers” from the semiconductor/dielectric interface can be controlled precisely. This unique method would provide us with an interesting experimental tool

**Received:** November 18, 2010

**Accepted:** January 24, 2011

**Published:** January 27, 2011

to construct OTFTs with the layers having different charge transport properties and to correlate them with the charge transport behaviors of OTFTs.

Figure 1 shows the structure of the transistors used in this study. Transistors with a channel length ( $L$ ) of  $50\ \mu\text{m}$  and width ( $W$ ) of  $3\ \text{mm}$  were fabricated in a bottom-gate configuration using highly doped Si as the gate electrode. A divinyltetramethyl-disiloxanebis (benzocyclobutene) (BCB) modified  $\text{SiO}_2$  layer was used as the gate dielectric. Chlorobenzene solutions (from  $0.25$  to  $4\ \text{g L}^{-1}$ ) of P3HT were directly spin-coated at  $600\ \text{rpm}$  onto the dielectric substrates, and then an  $11\ \text{nm}$  thick P3HT film was transferred by the CFT method on the top of the spin coated film. Briefly speaking, water-soluble polymers such as sodium poly(styrenesulfonate) (PSS) act as a “sacrificial layer” in the transfer process. A film with a structure of glass/PSS/P3HT was prepared by successive spin coating of an aqueous solution of PSS and a chlorobenzene solution of P3HT ( $2\ \text{g L}^{-1}$ ). This polymer film was gently brought into contact with the surface of the P3HT/BCB layer with the polymer face down. One drop of water was placed on the edge of the stacked substrates. After the water flowed from one side of the substrate to the other, the glass substrate was detached from the organic layer, resulting in the transfer of the polymer film from the glass to the surface of the P3HT/BCB layer. Note that the water selectively permeates into the PSS layer, not into the P3HT/P3HT interface because of the hydrophobic nature of the space. Gold electrodes were then evaporated onto the surface through a metal mask. The thickness of the P3HT layer was determined by X-ray reflectivity (XRR) measurements.

Since the film transfer is conducted in very mild conditions (without any heat, pressure, or organic solvents), the possibility of the intermixing of the two polymer layers is expected to be low. Before the film transfer, the surface of P3HT is very flat conformed by atomic force microscopy (AFM) (the roughness factor  $R_a$  was ca.  $0.3\ \text{nm}$ ), so the transferred interface could be flat at the same level, assuming the surface structures are preserved. We have never observed the delamination at the transferred interface, indicating strong van der Waals interaction at the interface. Although we cannot completely exclude the possibility of voids existing at the interface at this stage, reasonably high reproducibility of the device performance suggests the presence of a closely laminated interface.

Figure 2a shows carrier mobility  $\mu$  calculated from the source-drain current at  $V_G = -60\ \text{V}$  as a function of the thickness of the spin-coated P3HT film beneath the P3HT films transferred by CFT (see also Figure 1). For the device without a spin-coated film ( $0\ \text{nm}$ ), the average carrier mobility was  $0.086\ \text{cm}^2/(\text{V s})$  that coincides with our previous report.<sup>11</sup> When a spin-coated film existed between the dielectric layer and the transferred film, the carrier mobilities gradually decrease as the thickness of the spin coated films was increased, and the mobility converged to  $5 \times 10^{-4}\ \text{cm}^2/(\text{V s})$  at the thickness of ca.  $6\ \text{nm}$ . This mobility is consistent with the value in the spin-coated OTFT device without any transferred layer on the top ( $3 \times 10^{-4}\ \text{cm}^2/(\text{V s})$ ). This result can be qualitatively explained as follows: although most of the charge carriers (about 99% of total charges) is accumulated in the very first layer at the dielectric interface in this high  $|V_G|$  condition,<sup>13</sup> the buried surface layers at the transferred interface can still contribute to the apparent mobility until the thickness reached to around  $6\ \text{nm}$  because the buried surface layers have ca. 100 times higher intrinsic mobility than the bulk and polymer/substrate interface (see below).<sup>11</sup>

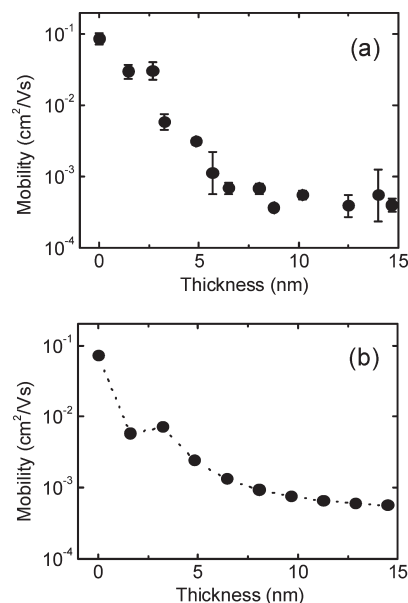


**Figure 2.** (a) Experimental and (b) calculated mobilities of the OTFT in the saturation regimes ( $V_G = -60\ \text{V}$ ) as a function of the thickness of the spin-coated P3HT film ( $0\ \text{nm}$  means the P3HT film was transferred directly onto the BCB layer).

Figure 3a shows the mobility dependence on  $V_G$  with the various thicknesses of the spin-coated films. For the device without the spin-coated film ( $0\ \text{nm}$ ), the mobility increased monotonically as  $|V_G|$  increased. This feature is usually observed in OTFTs prepared by solution process and vacuum evaporation, which can be explained by the trap filling effect as a result of the increase in the carrier concentration at high  $|V_G|$ .<sup>13–15</sup> Interestingly, the mobility shows an unusual dependence on  $V_G$  in the devices with the spin-coated P3HT films. When the spin-coated P3HT film was thin (less than  $4.9\ \text{nm}$  in Figure 3a), the carrier mobility first increased with  $|V_G|$  and then decreased. The higher carrier mobility at low  $|V_G|$  suggested that the inside part of the semiconductor film other than the semiconductor/dielectric interface could also significantly contribute to the current. This phenomenon was also observed in the OTFTs with single crystals and it was attributed to the faster charge transport in the bulk than at the interface due to the existence of structural defects at the surface of the single crystal.<sup>16</sup> It is noteworthy that the mobility with the spin-coated P3HT film of  $2.7\ \text{nm}$  was higher than that of the device without the spin-coated film ( $0\ \text{nm}$ ) at low  $|V_G|$  ( $<10\ \text{V}$ ) as indicated by a wide arrow in Figure 3a. This reversal of the mobility indicates that the buried surface layers could even play a major role for the apparent mobility of OTFT at low  $|V_G|$ . When the spin coated film was thicker (larger than  $8.8\ \text{nm}$  in Figure 3a), the carrier mobility showed first a rapid decrease and then the saturation as the  $|V_G|$  increased.

To analyze the thickness and  $V_G$  dependence of the mobility quantitatively, we need to consider both the charge carrier distribution in the films and the mobility dependence on the charge density. We first calculated the charge carrier distribution in the P3HT film according to the report by Horowitz et al.<sup>17</sup> We assumed that the semiconducting film consist of the stack of  $1.6\ \text{nm}$  thick layers, corresponding to the lamellar structure for P3HT.<sup>18</sup> Under the gradual channel approximation, the carrier distribution vertical to the dielectric interface was calculated with

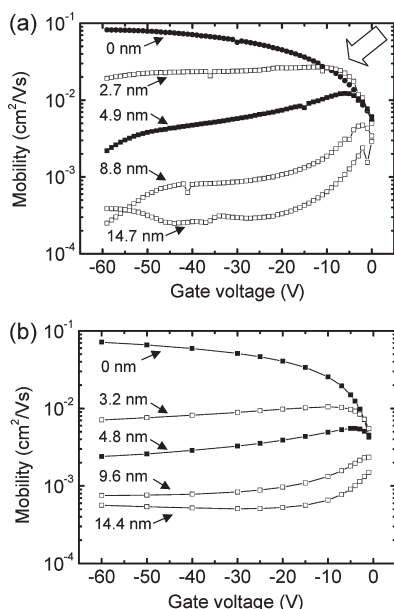


**Figure 3.** (a) Experimental and (b) calculated data of gate voltage dependence of the mobility in OTFT with the different thickness of the spin-coated P3HT films. (The thicknesses of the spin coated P3HT films are indicated inside the figures. 0 nm means the P3HT film was transferred directly onto the BCB layer). The broad arrow in a indicates the reversal of the apparent mobility at low  $V_G$  between the devices with of 0 and 2.7 nm thick films.

a capacitance  $C_i = 10.7 \text{ nF/cm}^2$  for the  $\text{SiO}_2/\text{BCB}$  dielectric layer and the relative dielectric constant of P3HT  $\epsilon_r = 3.9$ . Bar charts in Figures 4 show the calculated charge distributions with  $V_G$  of  $-5$  or  $-60$  V for 16 layers of P3HT (25.6 nm thick) as a function of the layer number 1 (closest to the dielectric interface) to 16. It can be seen that the most fraction of the charges accumulated in the first layer as  $|V_G|$  increased from 5 to 60 V, but 1% of the total charges still exists in the fifth layer (8 nm apart) from the dielectric interface even with  $V_G = -60$  V.

Next, the mobility dependence on the charge carrier density was considered by using a model developed by Vissenberg and Matters, which is based on carrier hopping between localized states.<sup>19</sup> According to this model, the local mobility  $\mu_l$  depends on the carrier density  $\rho$  following the expression

$$\mu_l = \frac{\sigma_0}{e} \left( \frac{\pi(T_0/T)^3}{(2\alpha)^3 B_c \Gamma(1-(T/T_0)) \Gamma(1+(T/T_0))} \right)^{T_0/T} \rho^{T_0/T-1} \quad (1)$$

where  $\sigma_0$  is the prefactor for the conductivity,  $\alpha^{-1}$  is effective overlap parameter between localized states,  $B_c$  is the critical number for the onset of percolation (set to 2.8 for 3D amorphous systems) and  $T_0$  is the width of the exponential distribution at the tail of density of states. Meijer et al. showed that this model could well-describe  $V_G$  dependence of the OTFT based on spin-coated P3HT with the experimental parameters  $T_0$ ,  $\sigma_0$ , and  $\alpha^{-1}$  that were extracted from the variable-temperature measurements.<sup>20</sup> We adapted the same parameter values for the charge transport in the bulk part and at the dielectric interface of P3HT ( $T_0 = 425$  K,  $\sigma_0 = 1.6 \times 10^6 \text{ S m}^{-1}$  and  $\alpha^{-1} = 1.6 \times 10^{10} \text{ m}$ ). We have extracted these parameters in the same way from the variable-temperature measurement on the OTFT based on the transferred

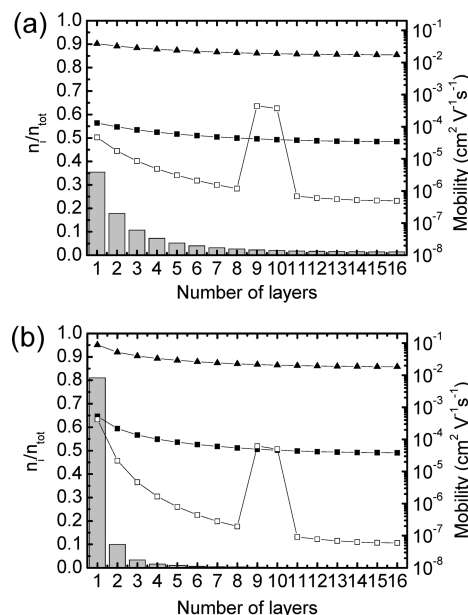


**Figure 4.** Calculated distribution of the charge carriers  $n_i/n_{\text{tot}}$  (bar charts, left axis), local carrier mobilities  $\mu_l$  of the buried surface layer (filled triangle, right axis) and those of the bulk of P3HT (filled square, right axis) and the product  $\mu_l \times n_i/n_{\text{tot}}$  (open square, right axis) in a P3HT film with 16 layers (25.6 nm thick) at  $V_G$  of (a)  $-5$  V and (b)  $-60$  V. The 1st layer is the closest to the dielectric layer, and it is assumed that the 9th and 10th layers have the mobility of the buried surface layer and the others have that of the bulk part. The calculated apparent mobilities for a) and b) are  $9.1 \times 10^{-4}$  and  $5.7 \times 10^{-4} \text{ cm}^2/(\text{V s})$ , respectively.

P3HT by CFT methods<sup>12</sup> and  $T_0 = 375$  K,  $\sigma_0 = 2.3 \times 10^6 \text{ S m}^{-1}$ , and  $\alpha^{-1} = 4.5 \times 10^{10} \text{ m}$  were obtained. The local mobilities calculated from the charge density and the above parameters with  $V_G$  of  $-5$  or  $-60$  V were plotted for the bulk part and the buried surface layers in Figure 4. In both case, moderate dependence of the local mobility on the charge carrier density was observed.

Taking both the factors into account, the apparent mobility  $\mu_{\text{app}}$  in the OTFTs is given by

$$\mu_{\text{app}} = \sum_{i=1}^L \mu_{li} \frac{n_i}{n_{\text{tot}}} \quad (2)$$

where  $L$  is the total layer numbers of the film,  $\mu_{li}$  is the local carrier mobility in  $i$ th layer, and  $n_i/n_{\text{tot}}$  is the distribution of charge carriers. In our model, two layers at the transferred interface (i.e., ninth and tenth layers in Figure 4) have the high mobility of the buried surface layers, and the other layers have low mobility of the bulk part. The product of  $\mu_{li}$  and  $n_i/n_{\text{tot}}$  is plotted in Figure 4. Equation 2 indicates that the sum of these mobilities in all the layers gives the apparent mobility  $\mu_{\text{app}}$ . We can see that the contribution of the buried surface layers at ninth and 10th layers to the apparent mobility is larger with  $V_G$  of  $-5$  V, but still visible with  $V_G$  of  $-60$  V.

The calculated apparent mobilities based on the above model were plotted as a function of the thickness of the spin-coated film (Figure 2b) and as a function of  $V_G$  (Figure 3b). Considering the simplicity of the model, the calculated results reproduce the experimental behaviors quite well: the limited thickness at which the effects of the transferred films diminish is about 6 nm with calculation in Figure 2b, which matches with the experimental data in Figure 2a. Figure 3b shows that the mobility increases

with  $|V_G|$  in the device with the transferred P3HT film, whereas with thin spin-coated films inserted, the mobility increases a little at first and start to decrease. Upon close inspection of Figure 3b, it can be seen that the reversal of the apparent mobility at low  $|V_G|$  observed in the experimental results is reproduced in the calculations (the mobilities of the devices with the spin-coated P3HT film of 3.2 and 0 nm at  $V_G$  of  $-1$  V are  $5.5 \times 10^{-3}$  and  $4.5 \times 10^{-3}$   $\text{cm}^2/(\text{V s})$ , respectively). When the spin-coated films get thicker than 9.6 nm (i.e., six layers), the carrier mobility decrease with  $|V_G|$  at first and then converged to a constant value. These agreements with the experimental observations also support the validity of the picture for the spin-coated P3HT films in which only the surface layer is well-ordered and constructs a charge transport path with much higher mobility than those of the bulk part and the dielectric interface.

In conclusion, we studied how the buried surface layers with high charge transport ability affect the OTFT characteristics by utilizing CFT methods. The results support that the surface layer of P3HT have higher carrier mobility than those in the bulk and at the polymer/substrate interface. They also showed that charge transport layers located far from the dielectric interface could contribute significantly to the total current in OTFT. This experimental method could be extended to various the model systems that would help to understand the complicated behaviors in OTFTs with the vertically inhomogeneous structures.

## AUTHOR INFORMATION

### Corresponding Author

\*E-mail: hashimoto@light.t.u-tokyo.ac.jp (K.Z.); k-tajima@light.t.u-tokyo.ac.jp (K.T.).

## REFERENCES

- (1) Bao, Z.; Locklin, J. *Organic Field-Effect Transistors*; CRC Press: Boca Raton, FL, 2007.
- (2) Fritz, S. E.; Martin, S. M.; Frisbie, C. D.; Ward, M. D.; Toney, M. F. *J. Am. Chem. Soc.* **2004**, *126*, 4084–4085.
- (3) Kline, R. J.; McGehee, M. D.; Toney, M. F. *Nat. Mater.* **2006**, *5*, 222–228.
- (4) Hao, X. T.; Hosokai, T.; Mitsuo, N.; Kera, S.; Okudaira, K. K.; Mase, K.; Ueno, N. *J. Phys. Chem. B* **2007**, *111*, 10365–10372.
- (5) Ho, P. K. H.; Chua, L. L.; Dipankar, M.; Gao, X. Y.; Qi, D. C.; Wee, A. T. S.; Chang, J. F.; Friend, R. H. *Adv. Mater.* **2007**, *19*, 215–221.
- (6) Ruiz, R.; Papadimitratos, A.; Mayer, A. C.; Malliaras, G. G. *Adv. Mater.* **2005**, *17*, 1795–1798.
- (7) Sirringhaus, H. *Adv. Mater.* **2009**, *21*, 3859–3873.
- (8) Kim, C.; Facchetti, A.; Marks, T. J. *Science* **2007**, *318*, 76–80.
- (9) Veres, J.; Ogier, S.; Lloyd, G.; de Leeuw, D. *Chem. Mater.* **2004**, *16*, 4543–4555.
- (10) Wei, Q.; Tajima, K.; Hashimoto, K. *ACS Appl. Mater. Interfaces* **2009**, *1*, 1865–1868.
- (11) Wei, Q. S.; Miyanishi, S.; Tajima, K.; Hashimoto, K. *ACS Appl. Mater. Interfaces* **2009**, *1*, 2660–2666.
- (12) Wei, Q. S.; Tajima, K.; Hashimoto, K. *Appl. Phys. Lett.* **2010**, *96*, 243301.
- (13) Tanase, C.; Meijer, E. J.; Blom, P. W. M.; de Leeuw, D. M. *Org. Electron.* **2003**, *4*, 33–37.
- (14) Horowitz, G.; Hajlaoui, R.; Fichou, D.; El Kassmi, A. *J. Appl. Phys.* **1999**, *85*, 3202–3206.
- (15) Horowitz, G.; Hajlaoui, M. E.; Hajlaoui, R. *J. Appl. Phys.* **2000**, *87*, 4456–4463.
- (16) Takeya, J.; Yamagishi, M.; Tominari, Y.; Hirahara, R.; Nakazawa, Y.; Nishikawa, T.; Kawase, T.; Shimoda, T.; Ogawa, S. *Appl. Phys. Lett.* **2007**, *90*.

- (17) Mottaghi, M.; Horowitz, G. *Org. Electron.* **2006**, *7*, 528–536.
- (18) Zhang, Y.; Tajima, K.; Hashimoto, K. *Macromolecules* **2009**, *42*, 7008–7015.
- (19) Vissenberg, M.; Matters, M. *Phys. Rev. B* **1998**, *57*, 12964–12967.
- (20) Meijer, E. J.; Tanase, C.; Blom, P. W. M.; van Veenendaal, E.; Huisman, B. H.; de Leeuw, D. M.; Klapwijk, T. M. *Appl. Phys. Lett.* **2002**, *80*, 3838–3840.